Syntheses and Superoxide Dismuting Activities of Partially (1−4) β-Chlorinated Derivatives of Manganese(III) *meso*-Tetrakis(*N*-ethylpyridinium-2-yl)porphyrin

Remy Kachadourian, Ines Batinić-Haberle, and Irwin Fridovich*

Department of Biochemistry, Duke University Medical Center, Durham, North Carolina 27710

Received July 28, 1998

Manganese(III) β-mono-, di-, tri-, and tetrachloro-5,10,15,20-tetrakis(*N*-ethylpyridinium-2-yl)porphyrin ($MnCl_x$-TE-2-PyP^{5+}, with *x* from 1 to 4) were prepared through β-chlorination of 5,10,15,20-tetrakis(2-pyridyl)porphyrin (H_2T-2-PyP) followed by *N*-ethylation and metallation. Metal centered redox potentials and superoxide dismutation activities were measured. Starting from MnTE-2-PyP^{5+}, whose redox potential and the related superoxide dismutation activity were $E°_{1/2} = +228$ mV *vs* NHE and $k_{cat} = 5.7 \times 10^7$ M^{-1} s^{-1}, respectively, the average increase of 55 mV in the redox potential per added chlorine was accompanied by a 65% increase in the rate constant. With $E°_{1/2} = +448$ mV, the tetrachlorinated derivative $MnCl_4$TE-2-PyP^{5+} exhibited the highest superoxide dismuting rate $k_{cat} = 4.0 \times 10^8$ M^{-1} s^{-1}. The relationship between the redox properties (thermodynamic and kinetic factors) and the superoxide dismuting activity of such compounds is discussed.

Introduction

Superoxide dismutase (SOD) is a metalloenzyme which catalyzes the dismutation of superoxide (O_2^-) into dioxygen (O_2) and hydrogen peroxide (H_2O_2).[1] The isolated SODs exhibit a redox potential reasonably close to +360 mV vs NHE, a value that is optimal for the dismutation reaction, with the same rate constants for each half reaction (2×10^9 M^{-1} s^{-1}) (Scheme 1).[2−4] Numerous diseases, including inflammations and reperfusion injuries, have been shown to involve overproduction of the superoxide radical, which explains the growing interest in the search for SOD mimics.[5] Several low-molecular-weight metal complexes including metallated cyclic polyamines and metalloporphyrins have already been found to be catalysts for the dismutation of superoxide.[6−9]

Metalloporphyrins have been investigated as catalysts for oxidation reactions as well as therapeutic agents, deoxyribonucleic acid (DNA) cleavers, and photosensitizers.[10] Introducing β electron-withdrawing substituents and modifying meso substituents on metalloporphyrins can have a major impact on their redox and electrostatic properties.[8,9] Thus, such substitutions facilitate tuning the redox potential of the metal center in order to approach the theoretically optimal redox potential for a superoxide dismuting catalyst, which, for instance, is between +200 and +500 mV. The β-octabrominated analogue of manganese(III) *meso*-tetrakis(*N*-methylpyridinium-4-yl)porphyrin (MnOBTMPyP^{4+}) exhibited a superoxide dismuting rate approximately 60-fold faster than its nonbrominated precursor MnTM-4-PyP^{5+}. The large positive redox potential of MnOBTMPyP^{4+} ($E°_{1/2} = +480$ mV *vs* NHE) stabilizes manganese in its 2+ state, which leads to Mn(II) dissociation.[8] On the other hand, the *ortho* analogue of MnTM-4-PyP^{5+}, MnTM-2-PyP^{5+} ($E°_{1/2} = +220$ mV *vs* NHE), was 16-fold more active and was a stable Mn(III) complex, as shown by its stability in the presence of excess EDTA.[9] In addition, the axial orientation of the *N*-methylpyridinium groups in MnTM-2-PyP^{5+} leads to a significantly lower degree of interaction with nucleic acids, which, in turn, causes this metalloporphyrin to be less toxic and therefore a more useful SOD mimic *in vivo*.[9] Moreover, preliminary experiments confirmed that the increase in the length of the *N*-alkyl substituent in MnTE-2-PyP^{5+} (*N*-ethyl instead of *N*-methyl), which introduces additional axial bulkiness into the molecule, further decreases the binding of the porphyrin to nucleic acids.[11]

Scheme 1[a]

O_2^-	⟶	$O_2 + e$	$E° = -160$ mV *vs* NHE[a]
$O_2^- + 2H^+ + e$	⟶	H_2O_2	$E° = +890$ mV *vs* NHE (pH 7)[a]
$2O_2^- + 2H^+$	⟶	$O_2 + H_2O_2$	*potential midway* $E°_{1/2} \sim +360$ mV

[a] Reference 2.

* Author for correspondence.

(1) Fridovich, I. *Annu. Rev. Biochem.* **1995**, *64*, 97.
(2) Ellerby, L. M.; Cabelli, D. E.; Graden, J. A.; Valentine J. S. *J. Am. Chem. Soc.* **1996**, *118*, 6556.
(3) Vance, C. K.; Miller, A.-F. *J. Am. Chem. Soc.* **1998**, *120*, 461.
(4) Klug-Roth, D.; Fridovich, I.; Rabani, J. *J. Am. Chem. Soc.* **1973**, *95*, 2786.
(5) (a) Gutteridge, J. M. C. *Free Radical Res. Commum.* **1993**, *19*, 141. (b) Keller, N. J.; Kindy, M. S.; Holtsberg, F. W.; St. Clair, D. K.; Yen, H.-C.; Germeyer, A.; Steiner, S. M.; Bruce-Keller, A. J.; Hutchins, J. B.; Mattson, M. P. *J. Neurosci.* **1998**, *18*, 687. (c) Kiningham, K. K.; St. Clair, D. K. *Cancer Res.* **1997**, *57*, 5265.
(6) (a) Zhang, D.; Busch, D. H.; Lennon, P. L.; Weiss, R. H.; Neumann W. L.; Riley, D. P. *Inorg. Chem.* **1998**, *37*, 956. (b) Faulkner, K. M.; Fridovich, I. *Handbook of Synthetic Antioxidants*; Packer, L., Cadenas, E., Eds.; Marcel Dekker: New York, 1997; p 375. (c) Rodriguez, M. C.; Morgenstern-Badarau, I.; Cesario, M.; Guilhem, J.; Keita, B.; Nadjo, L. *Inorg. Chem.* **1996**, *35*, 7804.
(7) Faulkner, K. M.; Liochev, S. I.; Fridovich, I. *J. Biol. Chem.* **1994**, *269*, 23471.
(8) Batinić-Haberle, I.; Liochev, S. I.; Spasojević, I.; Fridovich, I. *Arch. Biochem. Biophys.* **1997**, *343*, 225.
(9) Batinić-Haberle, I.; Benov, L.; Spasojević, I.; Fridovich, I. *J. Biol. Chem.* **1998**, *273*, 24521.
(10) (a) Meunier, B. *Chem. Rev.* **1992**, *92*, 1411. (b) Bonnett, R. *Chem. Soc. Rev.* **1995**, *24*, 19. (c) Cernay, T. H.; Zimmermann, H. W. *J. Photochem. Photobiol., B* **1996**, *34*, 191.
(11) Benov, L.; Kachadourian, R.; Batinić-Haberle, I.; Fridovich, I. Unpublished results.

10.1021/ic9808854 CCC: $18.00
Published on Web 12/23/1998

Complete β-halogenation of *meso*-tetraphenylporphyrin (H_2-TPP) and analogues has been extensively studied in order to obtain oxidation catalysts, but not many studies were devoted to the synthesis and physicochemical properties of partially halogenated porphyrins.[12−17] In the early seventies, Callot showed that the β-substitution was regioselective, but the structure of the main tetrahalogenated regioisomer, as the 7,8,-17,18 one, was confirmed only recently (12 regioisomers of the tetrasubstitution are theoretically allowed).[13−15] Introducing chlorine or bromine on β-pyrrole positions affects the redox potential of the porphyrin and its metal center in a similar fashion.[8,17] Yet, β-substitution with chlorine instead of with bromine would allow production of SOD mimics of lower molecular weight. In addition, less steric hindrance by the less bulky chlorine may lead to less distortion of the porphyrin ring and increased metal−ligand stability.[14,8] To increase the SOD-like activity of manganese(III) *meso*-tetrapyridinium porphyrins without sacrificing stability, but also to obtain a better understanding of the relationship between redox properties (thermodynamic and kinetic factors) and superoxide dismuting rate, we have prepared partially (1−4) β-chlorinated derivatives of MnTE-2-PyP^{5+} (MnCl$_x$TE-2-PyP^{5+}) (Figure 1).

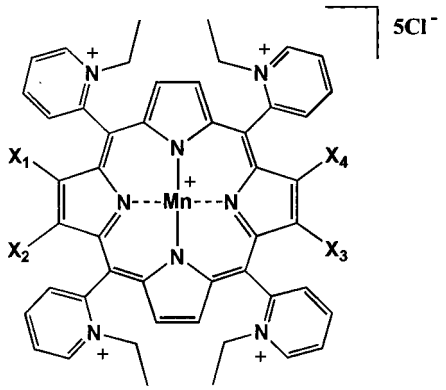

MnTE-2-PyP^{5+}	$X_1=X_2=X_3=X_4=H$
MnCl$_1$TE-2-PyP^{5+}	$X_1=Cl$, $X_2=X_3=X_4=H$
MnCl$_{2a}$TE-2-PyP^{5+}	$X_1=X_2=Cl$, $X_3=X_4=H$
MnCl$_3$TE-2-PyP^{5+}	$X_1=X_2=X_3=Cl$, $X_4=H$
MnCl$_4$TE-2-PyP^{5+}	$X_1=X_2=X_3=X_4=Cl$

Figure 1. Structures of MnCl$_x$TE-2-PyP^{5+} ($x = 1-4$).

Experimental Section

Materials. 5,10,15,20-Tetrakis(2-pyridyl)porphyrin (H_2T-2-PyP) was purchased from Mid-Century Chemicals (Posen, IL).[18] *N*-Chlorosuccinimide (NCS), ethyl-*p*-toluenesulfonate (ETS), tetrabutylammonium chloride (98%) (TBAC), ammonium hexafluorophosphate (NH_4PF_6), manganese chloride, sodium L-ascorbate (99%), cytochrome *c*, xanthine, ethylenedinitrilotetraacetic acid (EDTA), *N*,*N*-dimethylformamide (98.8%, anhydrous), and 2-propanol (99.5%) were from Sigma−Aldrich. Ethanol (absolute), acetone, ethyl ether (anhydrous), chloroform, and dichloromethane (HPLC grade) were from Mallinckrodt and were used without further purification. Xanthine oxidase was supplied by R. D. Wiley.[19] Thin-layer chromatography (TLC) plates (Baker-flex silica gel IB) were from J. T. Baker (Phillipsburg, NJ). Wakogel C-300 was from Wako Pure Industry Chemicals, Inc. (Richmond, VA).

Instrumentation. Proton nuclear magnetic resonance (^{1}H NMR) spectra were recorded on a Varian Inova 400 spectrometer. Ultraviolet−visible (UV−vis) spectra were recorded on a Shimadzu spectrophotometer model UV-260. Matrix-assisted laser desorption/ionization−time-of-flight (MALDI−TOFMS) and electrospray/ionization mass spectrometry (ESMS) were performed on Bruker Proflex III and Fisons Instruments VG Bio-Q triple quadrupole spectrometers, respectively.

H_2Cl$_1$T-2-PyP. H_2T-2-PyP (50 mg, 8.1×10^{-5} mol) was refluxed in chloroform with 43 mg (3.22×10^{-4} mol) of NCS.[14] The reaction was followed by normal-phase silica TLC using the mixture EtOH/CH_2Cl_2 (5:95) as eluant. After 6 h of reaction, the solution was washed once with distilled water. The chloroform was evaporated, and the products of the reaction were chromatographed over 100 g of Wakogel C-300 on a 2.5×50 cm column using the same eluant. The fraction corresponding to H_2Cl_1T-2-PyP was purified again using the same system, which leads to 16 mg of a black-purple solid (30%): TLC $R_f = 0.47$; UV−vis ($CHCl_3$) λ_{nm} (log ϵ) 419.6 (5.44), 515.2 (4.21), 590.0 (3.72), 645.8 (3.25); MALDI−TOFMS *m*/*z* 654 (M + H$^+$); ^{1}H NMR ($CDCl_3$) δ_{ppm} −2.91 (2H, NH), 7.66−7.74 (m, 4H), 7.99−8.21 (m, 8H), 7.68 (s, 1H), 8.74 (d, 1H, $J = 6$ Hz), 8.76 (d, 1H, $J = 6$ Hz), 8.76 (d, 1H, $J = 6$ Hz), 8.88 (d, 1H, $J = 6$ Hz), 8.90 (d, 1H, $J = 6$ Hz), 8.94 (d, 1H, $J = 6$ Hz), 9.04−9.14 (m, 4H).

H_2Cl$_{2a}$T-2-PyP. The same procedure as described above leads to 5.3 mg of a black-purple solid (10%): TLC $R_f = 0.50$; UV−vis ($CHCl_3$) λ_{nm} (log ϵ) 421.4 (5.38), 517.8 (4.21), 591.4 (3.78), 647.6 (3.51); MALDI−TOFMS *m*/*z* 688 (M + H$^+$); ^{1}H NMR ($CDCl_3$) δ_{ppm} −2.98 (2H, NH), 7.66−7.74 (m, 4H), 8.00−8.20 (m, 8H), 8.70 (s, 2H), 8.82 (d, 2H, $J = 6$ Hz), 8.91 (d, 2H, $J = 6$ Hz), 9.06−9.14 (m, 4H).

H_2Cl$_{2b+2c}$T-2-PyP. The same procedure leads to 11 mg of a black-purple solid (20%): TLC $R_f = 0.53$; UV−vis ($CHCl_3$) λ_{nm} (log ϵ) 421.4 (5.42), 516.8 (4.25), 593.2 (3.74), 646.2 (3.31); MALDI-TOFMS *m*/*z* 688 (M + H$^+$); ^{1}H NMR ($CDCl_3$) δ_{ppm} −3.04 (2H, NH), −2.84 (1H, NH), −2.87 (1H, NH), 7.66−7.74 (m, 8H), 7.98−8.20 (m, 16H), 8.59 (s, 1H), 8.61 (s, 1H), 8.73 (d, 2H, $J < 2$ Hz), 8.78 (d, 2H, $J = 6$ Hz), 8.87 (d, 2H, $J = 6$ Hz), 8.93 (d, 2H, $J < 2$ Hz), 9.02−9.14 (m, 8H).

H_2Cl$_3$T-2-PyP. The same procedure, using 65 mg (4.87×10^{-4} mol) of NCS, leads to 8.4 mg of a black-purple solid (14%): TLC $R_f = 0.55$; UV−vis ($CHCl_3$) λ_{nm} (log ϵ) 422.8 (5.37), 519.4 (4.21), 593.8 (3.71), 651.4 (3.37); MALDI−TOFMS *m*/*z* = 723 (M + H$^+$); ^{1}H NMR ($CDCl_3$) δ_{ppm} −3.08 (1H, NH), −3.15 (1H, NH), 7.66−7.74 (m, 4H), 8.00−8.18 (m, 8H), 8.56 (s, 1H), 8.72 (d, 1H, $J = 6$ Hz), 8.76 (d, 1H, $J = 6$ Hz), 8.82 (d, 1H, $J = 6$ Hz), 8.88 (d, 1H, $J = 6$ Hz), 9.04−9.14 (m, 4H).

H_2Cl$_4$T-2-PyP. The same procedure, using 65 mg (4.87×10^{-4} mol) of NCS, leads to 7.3 mg of a black-purple solid (12%): TLC $R_f = 0.58$; UV−vis ($CHCl_3$) λ_{nm} (log ϵ) 423.4 (5.33), 520.0 (4.19), 595.6 (3.66), 651.0 (3.33); MALDI−TOFMS *m*/*z* = 758 (M + H$^+$); ^{1}H NMR ($CDCl_3$) δ_{ppm} −3.14 (2H, NH), 7.66−7.74 (m, 4H), 7.98−8.16 (m, 8H), 8.74 (d, 4H, $J < 2$ Hz), 9.06−9.12 (m, 4H).

(12) (a) Hoffmann, P.; Robert, A.; Meunier B. *Bull. Soc. Chim. Fr*. **1992**, *129*, 85. (b) Chorghade, M. S.; Dolphin, D.; Dupre, D.; Hill, D. R.; Lee, E. C.; Wijesekera, T. *Synthesis* **1996**, 1320. (c) Wijesekera, T.; Dupre, D.; Cader, M. S. R.; Dolphin, D. *Bull. Soc. Chim. Fr*. **1996**, *133*, 765.

(13) (a) Callot, H. J. *Tetrahedron Lett*. **1973**, 4987. (b) Callot, H. J. *Bull. Soc. Chim. Fr*. **1974**, *7*−*8*, 1492.

(14) Ochsenbein, P.; Ayougou, K.; Mandon, D.; Fischer, J.; Weiss, R.; Austin, R. N.; Jayaraj, K.; Gold, A.; Terner, J.; Fajer J. *Angew. Chem., Int. Ed. Engl*. **1994**, *33*, 348.

(15) Crossley, M. J.; Burn, P. L.; Chew, S. S.; Cuttance, F. B.; Newsom, I. A. *J. Chem. Soc., Chem. Commun*. **1991**, 1564.

(16) (a) D'Souza, F.; Villard, A.; Van Caemelbecke, E.; Franzen, M.; Boschi, T.; Tagliatesta, P.; Kadish, K. M. *Inorg. Chem*. **1993**, *32*, 4042. (b) Chan, K. S.; Zhou, X.; Luo, B.-S.; Mak, T. C. W. *J. Chem. Soc., Chem. Commun*. **1994**, 271. (c) Chan, K. S.; Zhou, X.; Au, M. T.; Tam, C. Y. *Tetrahedron* **1995**, *51*, 3129. (d) Zhou, X.; Tse, M. K.; Wan, T. S. M.; Chan, K. S. *J. Org. Chem*. **1996**, *61*, 3590.

(17) (a) Sen, A.; Krishnan, V. *J. Chem. Soc., Faraday Trans*. **1997**, *93*, 4281. (b) Autret, M.; Ou, Z.; Boshi, A.; Tagliatesta, P.; Kadish, K. M. *J. Chem. Soc., Dalton Trans*. **1996**, 2793. (c) Hariprasad, G.; Dahal, S.; Maiya, B. G. *J. Chem. Soc., Dalton Trans*. **1996**, 3429. (d) Tagliatesta, P.; Li, J.; Autret, M.; Van Caemelbecke, E.; Villard, A.; D'Souza, F.; Kadish, K. M. *Inorg. Chem*. **1996**, *35*, 5570. (e) Ghosh, A. *J. Am. Chem. Soc*. **1995**, *117*, 4691. (f) Takeuchi, T.; Gray, H. B.; Goddard, W. A. *J. Am. Chem. Soc*. **1994**, *116*, 9730. (g) Binstead, R. A.; Crossley, M. J.; Hush, N. S. *Inorg. Chem*. **1991**, *30*, 1259. (h) Giraudeau, A.; Callot, H. J.; Jordan, J.; Ezhar, I.; Gross, M. *J. Am. Chem. Soc*. **1979**, *101*, 3857.

(18) Torrens, M.; Straub, D. K.; Epstein, L. M. *J. Am. Chem. Soc*. **1972**, *94*, 4160.

(19) Waud, W. R.; Brady, F. O.; Wiley, R. D.; Rajagopalan, K. V. *Arch. Biochem. Biophys*. **1975**, *19*, 695.

MnTE-2-PyP^{5+}. One-hundred milligrams (1.62×10^{-4} mol) of H_2T-2-PyP was dissolved in 5 mL of warm DMF (anhydrous), and 5.5 mL (3.22×10^{-2} mol) of ethyl-*p*-toluenesulfonate (ETS) was added under stirring at 90 °C and allowed to react for 24−48 h. The completion of tetra-*N*-ethylation was followed by normal-phase silica TLC using the mixture $KNO_{3sat}/H_2O/CH_3CN$ (1:1:8) as eluant.[9] Upon the completion of the reaction, the DMF was removed in vacuo, and 5 mL of acetone was then added. A concentrated solution of tetrabutylammonium chloride (TBAC) in acetone (∼1 g/10 mL of acetone) was added dropwise under stirring to this solution until precipitation of the chloride was complete. The resulting purple solid was dissolved in 10 mL of water, the pH of the solution was raised to 12 with NaOH, and 640 mg of $MnCl_2 \cdot 4H_2O$ (3.23×10^{-3} mol) was added.[9] Upon completion of metallation, the pH was lowered to between 4 and 7 in order to facilitate the autooxidation of Mn(II) into Mn(III), and the excess of metal was eliminated as follows. The solution was filtered, and a concentrated aqueous solution of NH_4PF_6 was added to precipitate the metalloporphyrin as the PF_6^- salt.[8,20] The precipitate was thoroughly washed with the mixture 2-propanol/ethyl ether (1:1) and dried in vacuo at room temperature. The resulting solid was then dissolved in acetone, and a concentrated solution of TBAC was added to isolate the metalloporphyrin in the form of its chloride salt. The precipitate was washed thoroughly with acetone and dried in vacuo at room temperature, leading to the formation of 150 mg of a black-red solid (95%): TLC $R_f = 0.18$; UV−vis (H_2O) λ_{nm} (log ϵ) 364.0 (4.64), 453.8 (5.14), 558.6 (4.05); ESMS *m*/*z* 157.4 (M^{5+}/5). Anal. Calcd for $MnC_{48}N_8H_{44}Cl_5 \cdot 5H_2O$: C, 54.64; H, 5.16; N, 10.62. Found: C, 54.55; H, 5.40; N, 10.39.

MnCl$_1$TE-2-PyP^{5+}. The same procedure as described above starting from 10 mg (1.53×10^{-5} mol) of H_2Cl_1T-2-PyP and 0.5 mL (2.94×10^{-3} mol) of ETS in 1 mL of DMF was performed to obtain the product: TLC $R_f = 0.20$; UV−vis (H_2O) λ_{nm} (log ϵ) 365.6 (4.63), 455.6 (5.13), 560.6 (4.02); ESMS *m*/*z* 164.3 (M^{5+}/5). Anal. Calcd for $MnC_{48}N_8H_{43}Cl_6 \cdot 5H_2O$: C, 52.91; H, 4.90; N, 10.28. Found: C, 52.59; H, 5.28; N, 10.14.

MnCl$_{2a}$TE-2-PyP^{5+}. The same procedure, starting from 5 mg (7.28×10^{-6} mol) of H_2Cl_{2a}T-2-PyP and 0.25 mL (1.47×10^{-3} mol) of ETS, leads to 7.5 mg of a black-red solid (95%): TLC $R_f = 0.21$; UV−vis (H_2O) λ_{nm} (log ϵ) 365.8 (4.58), 456.4 (5.05), 562.2 (4.00); ESMS *m*/*z* 171.1 (M^{5+}/5). Anal. Calcd for $MnC_{48}N_8H_{42}Cl_7 \cdot 6H_2O$: C, 50.48; H, 4.77; N, 9.81. Found: C, 50.08; H, 4.60; N, 10.01.

MnCl$_{2b+2c}$TE-2-PyP^{5+}. The same procedure, starting from 5 mg (7.28×10^{-6} mol) of H_2Cl_{2b+2c}T-2-PyP, leads to the formation of 7.5 mg of a black-red solid (95%): TLC $R_f = 0.22$; UV−vis (H_2O) λ_{nm} (log ϵ) 365.2 (4.63), 457.4 (5.08), 462.2 (4.06); ESMS *m*/*z* 171.1 (M^{5+}/5). Anal. Calcd for $MnC_{48}N_8H_{42}Cl_7 \cdot 5H_2O$: C, 51.29; H, 4.66; N, 9.97. Found: C, 51.31; H, 5.19; N, 9.68.

MnCl$_3$TE-2-PyP^{5+}. The same procedure, starting from 5 mg (6.93×10^{-6} mol) of H_2Cl_3T-2-PyP, leads to the formation of 7.5 mg of a black-brown solid (95%): TLC $R_f = 0.23$; UV−vis (H_2O) λ_{nm} (log ϵ) 364.8 (4.58), 458.0 (4.98), 466.4 (4.00); ESMS *m*/*z* 178.1 (M^{5+}/5). Anal. Calcd for $MnC_{48}N_8H_{41}Cl_8 \cdot 6H_2O$: C, 49.00; H, 4.54; N, 9.52. Found: C, 48.40; H, 4.26; N, 9.59.

MnCl$_4$TE-2-PyP^{5+}. The same procedure, starting from 5 mg (6.61×10^{-6} mol) of H_2Cl_4T-2-PyP, leads to the formation of 7.5 mg of a black-brown solid (95%): TLC $R_f = 0.24$; UV−vis (H_2O) λ_{nm} (log ϵ) 365.8 (4.52), 459.2 (4.90), 567.0 (3.96); ESMS *m*/*z* 184.9 (M^{5+}/5). Anal. Calcd for $MnC_{48}N_8H_{40}Cl_9 \cdot 5H_2O$: C, 48.33; H, 4.22; N, 9.39. Found: C, 48.38; H, 4.45; N, 9.53.

Electrochemistry. The electrochemical characterization was performed as described previously on a Voltammetric Analyzer model 600 (CH Instrument).[9,21] A 3-electrode setup system in a small-volume cell (0.5 mL), consisting of a 3-mm-in-diameter button glassy carbon working electrode (Bioanalytical Systems), a standard Ag/AgCl reference electrode, and a 0.5-mm platinum wire as an auxiliary electrode, was used. The samples were solutions containing 0.5 mM metalloporphyrin and 0.1 M NaCl in a 0.05 M phosphate buffer (pH 7.8). Scan rates were 10−500 mV/s, typically 100 mV/s, and the potentials were standardized against potassium ferricyanide/potassium ferrocyanide couple.[21]

Scheme 2

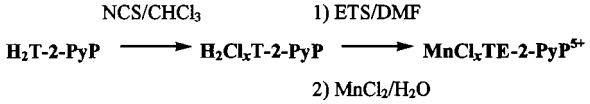

Table 1. H_2Cl_xT-2-PyP ($x = 1-4$): R_f, Soret Band Data and Yields with 4 and 6 Equiv of NCS

			Yield[c] (%)	
porphyrin	R_f [a]	λ[b] (nm)(ϵ/10^5 M^{-1} cm^{-1})	4 equiv	6 equiv
H_2T-2-PyP	0.43	418.4		
β-Cl$_1$	0.47	419.6 (2.74)	30	
β-Cl$_{2a}$	0.50	421.4 (2.39)	10	5
β-Cl$_{2b+2c}$	0.53	421.4 (2.62)	20	10
β-Cl$_3$	0.55	422.8 (2.33)	10	15
β-Cl$_4$	0.58	423.6 (2.13)	7	12

[a] TLC on silica with $EtOH/CH_2Cl_2$ (5:95) as eluant. [b] In $CHCl_3$ (estimated errors for ϵ are within ±10%). [c] In refluxing $CHCl_3$ during 6 h ($c \approx 2$ μM).

Superoxide Dismuting Activity. The SOD-like activities were measured using the xanthine/xanthine oxidase system as a source of O_2^- and ferricytochrome *c* as its indicating scavenger.[22] O_2^- was produced at the rate of 1.2 μM/min, and reduction of ferricytochrome *c* was followed at 550 nm. Assays were conducted in the presence of 0.1 mM EDTA in 0.05 M phosphate buffer (pH 7.8). Rate constants for the reaction of the compounds were found on the basis of competition with 10 μM cytochrome *c*, $k_{cyt\ c} = 2.6 \times 10^5$ M^{-1} s^{-1}.[23] All measurements were done at 25 °C. Cytochrome *c* concentration was at least 1000-fold higher than the concentrations of the SOD mimics, and the rates were linear for at least 2 min, during which the compounds intercepted ∼100 equivs of O_2^-, thus confirming the catalytic nature of O_2^- dismutation in the presence of the mimics.

Results and Discussion

Despite increasing knowledge of the purification of water soluble porphyrins, the separation of halogenated, uncharged porphyrins followed by *N*-alkylation and metallation still appeared easier for the successful preparation of $MnCl_x$TE-2-PyP^{5+} (Scheme 2).[20,24]

Synthesis of H_2T-2-PyP β-Chlorinated Derivatives. β-Chlorination of H_2T-2-PyP was performed as described in the literature for H_2TPP analogues, using *N*-chlorosuccinimide (NCS) in chloroform under refluxing conditions.[14] The number of NCS equivalents used can be 4 or 6, depending on the degree of substitution desired (Table 1). The reaction can be followed by TLC (silica gel) using a mixture of ethanol/dichloromethane (5:95) as eluant (Table 1 and Scheme 3). Each compound was purified by chromatography on silica gel (Wakogel C-300) using the same eluant. The structures of the main isomers were identified by mass spectrometry and UV−vis and ^{1}H NMR spectroscopies (Table 1 and Scheme 3). The bathochromic shift of the Soret band per chlorine on H_2T-2-PyP was only 1.3 nm compared to 3.5 nm, as reported previously for H_2TPP derivatives (Table 1).[12] Only one of the three dichlorinated regioisomers (β-Cl$_{2a}$ derivative) was purified by chromatography on silica gel. The two other regioisomers (β-Cl$_{2b}$ and β-Cl$_{2c}$ derivatives) did not differ in R_f. Preliminary results showed that

(20) Richards, R. A.; Hammons, K.; Joe, M.; Miskelly, G. M. *Inorg. Chem.* **1996**, *35*, 1940.
(21) Kolthof, I. M.; Tomsicek, W. J. *J. Phys. Chem.* **1974**, *39*, 945.
(22) McCord, J. M.; Fridovich, I. *J. Biol. Chem.* **1969**, *244*, 6049.
(23) Butler, J.; Koppenol, W. H.; Margoliash, E. J. *J. Biol. Chem.* **1982**, *257*, 10747.
(24) Kaufmann, T.; Shamsai, B.; Song Lu, R.; Miskelly, G. M. *Inorg. Chem.* **1995**, *34*, 5073.

Scheme 3

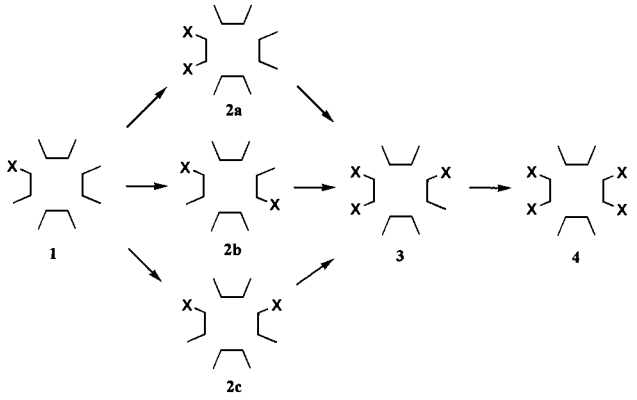

Table 2. H_2Cl_xT-2-PyP ($x = 1-4$): ^{1}H-NMR Data (Porphyrin Ring) in $CDCl_3$

		δ_{ppm}[a] (mult, Hz)
H_2Cl_1T-2-PyP	NH	−2.91 (2H)
	CH	7.68 (s, 1H)
		8.74 (d, 1H, 5.5)
		8.76 (d, 1H, 5.5)
		8.76 (d, 1H, 6.0)
		8.88 (d, 1H, 6.0)
		8.90 (d, 1H, 6.0)
		8.94 (d, 1H, 6.0)
$H_2Cl_{2a}T$-2-PyP	NH	−2.98 (2H)
	CH	8.70 (s, 2H)
		8.82 (d, 2H, 6.0)
		8.91 (d, 2H, 6.0)
$H_2Cl_{2b}T$-2-PyP[b]	NH	−3.04 (2H)
	CH	8.59 (s, 2H)
		8.78 (d, 2H, 6.0)
		8.87 (d, 2H, 6.0)
$H_2Cl_{2c}T$-2-PyP[b]	NH	−2.84 (1H)
		−2.87 (1H)
	CH	8.61 (s, 2H)
		8.73 (d, 2H, <2.0)
		8.93 (d, 2H, <2.0)
H_2Cl_3T-2-PyP	NH	−3.08 (1H)
		−3.15 (1H)
	CH	8.56 (s, 1H)
		8.72 (d, 1H, 6.5)
		8.76 (d, 1H, 6.5)
		8.82 (d, 1H, 6.5)
		8.88 (d, 1H, 6.5)
H_2Cl_4T-2-PyP	NH	−3.14 (2H)
	CH	8.74 (d, 4H, <2.0)

[a] Chemical shifts in ppm expressed relative to TMS by setting $CDCl_3$ = 7.24 ppm. [b] One spectrum for the mixture of the two regioisomers (~1:1 ratio).

purification of H_2Br_xT-4-PyP ($x = 1$ to 4) is more difficult. Indeed, using the same TLC system, β-Br_1 and β-Br_{2a} derivatives both have the same R_f, and no difference in R_f between β-Br_{2b}, β-Br_{2c}, β-Br_3, and β-Br_4 derivatives was observed, showing clearly that in this case R_f depends on the number of pyrroles substituted and not on the number of β-protons substituted (unpublished results).

^{1}H NMR Identification of H_2T-2-PyP β-Chlorinated Derivatives. ^{1}H NMR allowed the identification of the products of the substitution reaction (Table 2 and Figure 2). As described in the literature for H_2TPP analogues, the main regioisomer of H_2Cl_4T-2-PyP has chlorines in positions 7, 8, 17, and 18. Indeed, its ^{1}H NMR spectrum shows an apparent singlet (doublet with $J < 2$ Hz), corresponding to four chemically equivalent β-protons coupled with the two pyrrolic protons which have

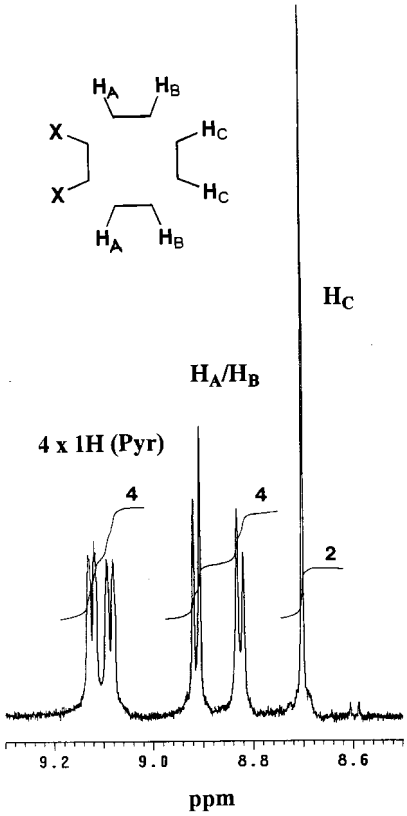

Figure 2. ^{1}H NMR spectrum (porphyrin ring) of H_2Cl_{2a}T-2-PyP in $CDCl_3$ (δ = 7.24 ppm). The four protons in α position to the four pyridyl nitrogens are taken as integration references.

lost their delocalization.[15] Nevertheless, another less polar fraction ($R_f = 0.60$) was identified, according to its mass spectrum, as a mixture of other tetrachloro regioisomers (^{1}H NMR spectrum uninterpretable), representing approximately 50 wt % of both β-Cl_4 fractions and showing that the β-substitution is only partially regioselective. According to the ^{1}H NMR spectrum of the corresponding H_2Cl_3T-2-PyP^{5+} fraction, there are no apparent other regioisomers. The spectrum presents one singlet corresponding to the β-proton of the monosubstituted pyrrole and four doublets corresponding to the four β-protons of the two nonsubstituted pyrroles. Moreover, the asymmetry of this compound leads to a differentiation of the two NH protons. According to yields and ^{1}H NMR spectra of H_2Cl_{2a}T-2-PyP (Figure 2) and H_2Cl_{2b+2c}T-2-PyP, no predominant β-Cl_2 regioisomer was observed. Finally, the H_2Cl_1T-2-PyP spectrum shows one singlet and six doublets but only one NH signal, suggesting that in this case the asymmetry is too weak for the differentiation of the two NH protons.

***N*-Ethylation and Metallation.** The *N*-ethylation of H_2T-2-PyP was efficiently accomplished using ethyl-*p*-toluenesulfonate, diethyl sulfate, or iodoethane as reagents, but the high toxicity of diethyl sulfate and the low reactivity of iodoethane makes ethyl-*p*-toluenesulfonate (ETS) the best choice.[25,26] Some authors prefer performing *N*-alkylation after metallation in order to protect the pyrrole nitrogens.[26] However, with direct treatment on our free ligands, no *N*-ethylation of the pyrrole nitrogens

(25) (a) Chen, S.-M.; Su, Y. O. *J. Electroanal. Chem.* **1990**, *280*, 189. (b) Kalyanasundaram, K. *Inorg. Chem.* **1984**, *23*, 2453. (c) Hambright, P.; Gore, T.; Burton, M. *Inorg. Chem.* **1976**, *15*, 1314. (d) Alder, R. W.; Sinnott, M. L.; Whiting, M. C.; Evans, D. A. *Chem. Br.* **1978**, *14*, 324.

(26) Perrée-Fauvet, M.; Verchere-Béaur, C.; Tarnaud, E.; Anneheim-Herbelin, G.; Bone, N.; Gaudemer, A. *Tetrahedron* **1996**, *52*, 13569.

Table 3. $MnCl_x$TE-2-PyP^{5+} ($x = 1-4$): Soret Band Data, Redox Potentials, and SOD Activities

Mn porphyrin	λ^a (nm) ($\epsilon/10^4$ M^{-1} cm^{-1})	$E°_{1/2}{}^b$ (Δ)	$IC_{50}{}^c/10^{-9}$ M	k_{cat} /10^7 M^{-1} s^{-1}
MnTE-2-PyP^{5+}	453.8 (14.0)	+228 (71)	45	5.7
β-Cl_1	455.6 (12.5)	+293 (65)	25	10
β-Cl_{2a}	456.4 (10.6)	+342 (70)	20	13
β-Cl_{2b+2c}	457.4 (11.2)	+344 (65)	20	13
β-Cl_3	458.0 (9.5)	+408 (67)	10	26
β-Cl_4	459.2 (8.0)	+448 (79)	6.5	40
MnTM-4-PyP^{5+}		+60		0.4[d]
MnTM-2-PyP^{5+}		+220		6.0[e]
MnOBTMPyP^{4+}		+480		22[f]
Cu,ZnSOD		+260		200[g]

[a] In H_2O (estimated errors for ϵ are within ±10%). [b] mV *vs* NHE, with estimated errors of ±5 mV (Δ = peak to peak separation), and in the following conditions: 0.5 mM porphyrin, 0.1 M NaCl, 0.05 M phosphate buffer (pH 7.8). [c] Concentration that causes 50% inhibition of cytochrome *c* reduction by O_2^- (estimated errors are within ±10%). [d] Reference 7. [e] Reference 9. [f] Reference 8. [g] Reference 4.

was observed (subsequent metallation in aqueous solution was complete). The completion of ethylation as well as metalation can be followed by TLC (normal silica) using a highly polar eluant, a mixture of an aqueous solution of saturated potassium nitrate with acetonitrile.[9] The yields of this step (*N*-ethylation and metallation) were almost 100% (approximately 5% loss during the purification process). Since *N*-ethylation (or *N*-methylation) limits the free rotation of the pyridinium rings, each compound is, in fact, a mixture of four atropoisomers, and a further purification of each atropoisomer can be considered.[24] All the manganese porphyrins prepared had metal in the 3+ state as demonstrated by the 20-nm hypsochromic shift of the Soret band (accompanied by the loss of splitting) upon the reduction of the metal center by ascorbic acid.

Electrochemistry. The metal-centered redox behavior of all metalloporphyrin products was reversible. The half-wave potentials ($E°_{1/2}$) were calculated as the average of the cathodic and anodic peaks and are given in mV *vs* NHE (Table 3). The average shift per chlorine is +55 mV (Table 3), which is in agreement with the values previously reported for H_2TPP derivatives (between +50 and +70 mV).[17] This shift appears to be higher (~+65 mV) between 0 and 1 and between 2 and 3 chlorines (Table 3). $E°_{1/2}$ values of β-Cl_{2a} and the mixture β-Cl_{2b+2c} were not significantly different. The manganese redox states of $MnCl_4$TE-2-PyP^{5+} ($E°_{1/2}$ = +448 mV) and MnOBTMPyP^{4+} ($E°_{1/2}$ = +480 mV) are 3+ and 2+, respectively; this difference may be explained by their difference in terms of redox potential (~30 mV) but also by structural considerations, for instance, an increased distortion of the porphyrin ring in the case of MnOBTMPyP^{4+}.[8,14]

Superoxide Dismuting Activities. SOD-like activities were measured as described previously, on the basis of competition with cytochrome *c*.[22] $MnCl_x$TE-2-PyP^{5+} SOD-like activities, both IC_{50} (M) and k_{cat} (M^{-1} s^{-1}) values, are reported in Table 3; IC_{50} (measured) represents the concentration for one unit of activity (or the concentration that causes 50% inhibition of the reduction of cytochrome *c* by O_2^-) and k_{cat} (calculated from IC_{50}) represents the rate constant for the superoxide dismutation reaction. Starting from MnTE-2-PyP^{5+}, the average increase in rate constant per added chlorine is 65%. The rate constant of $MnCl_4$TE-2-PyP^{5+} is approximately 2-, 7-, and 100-fold higher than MnOBTMPyP^{4+}, MnTM-2-PyP^{5+}, and MnTM-4-PyP^{5+}, respectively, corresponding to 20% of the activity of the Cu,Zn-SOD enzyme on a molar basis (40% per active site considering that the enzyme has two active sites).[7−9,4]

Test of Stability. Each additional degree of chlorination increases the redox potential, which is expected to be followed by the decrease in the pK_a values of pyrrole nitrogens, as found for the series of *meso*-phenyl- and *meso*-pyridyl-substituted porphyrins as well as for β-substituted ones.[27] The pK_a, as a measure of the ligand−proton stability, is, in turn, a measure of the metal−ligand stability as well. Thus, the tetrachloro compound is expected to be of decreased stability as compared to lesser chlorinated analogues. The stability of $MnCl_4$TE-2-PyP^{5+} was tested by measuring its SOD-like activity in the presence of excess EDTA. In the presence of a 100-fold excess of EDTA, $MnCl_4$TE-2-PyP^{5+} ($c = 5 \times 10^{-6}$ M) maintains its activity for 16 hours (at 25 °C). A loss of activity (~25%) was observed after 40 hours, thus indicating the formation of manganese−EDTA complex ($K = 10^{14.05}$). These results confirm a relatively good stability of $MnCl_4$TE-2-PyP^{5+} as compared to MnOBTMPyP^{4+} ($K = 10^{8.08}$).[8]

Relationship between Redox Properties and SOD-Like Activities. The Cu,Zn-SOD enzyme is a dimer of two identical subunits and, thus, has two active sites, which exhibit a redox potential close to the midpoint of the two half-reaction values, as well as the same rate constants for each half reaction (Scheme 1 and Table 3).[2,4] On the other hand, previous studies of O_2^- dismutation catalyzed by MnTM-4-PyP^{5+} ($E°_{1/2}$ = +60 mV), using pulse radiolysis and stopped-flow techniques, showed that the rate of the reduction of the metal by O_2^- is 100-fold to 1000-fold lower than the rate of reoxidation of the metal.[28] Whereas a peak of SOD-like activity somewhere between +200 and +450 mV was first expected, plotting k_{cat} *vs* $E°_{1/2}$ for $MnCl_x$TE-2-PyP^{5+} shows an exponential increase of the SOD-like activity (not shown), strongly suggesting that the limiting factor is still kinetic, i.e., the reduction of the metal center by O_2^-. This hypothesis, however, must be confirmed by measuring the rates of each half-reaction as catalyzed by each $MnCl_x$TE-2-PyP^{5+} compound. The relationship between activation free energy ($\Delta G^‡$) for superoxide dismutation and free energy change ($\Delta G°$) for $MnCl_x$TE-2-PyP^{5+} redox appears to be linear, and according to this behavior, activity equivalent to that of the Cu,Zn-SOD enzyme ($k_{cat} = 10^9$ M^{-1} s^{-1} per active site) might be reached at approximately $E°_{1/2}$ = +570 mV (Figure 3). Nevertheless, due to both steric (distortion of the porphyrin ring) and thermodynamic factors, introducing a higher degree of β-chlorination is expected to stabilize the manganese in the 2+

(27) (a) Worthington, P.; Hambright, P.; Williams, R. F.; Feldman, M. R.; Smith, K. M.; Langry, K. C. *Inorg. Nucl. Chem. Lett.* **1980**, *16*, 441. (b) Kadish, K. M.; Morrison, M. M. *Inorg. Chem.* **1976**, *15*, 980. (c) Batinić-Haberle, I.; Hambright, P.; Crumbliss, A. L.; Spasojević, I.; Fridovich, I. Manuscript in preparation.

(28) (a) Faraggi, M. *Oxygen Radicals in Chemistry and Biology;* Bors, W., Saran, M., Tait, D., Eds.; Walter de Gruyter and Co.: Berlin, Germany, 1984; p 419. (b) Lee, J.; Hunt, J. A.; Groves, J. T. *J. Am. Chem. Soc.* **1998**, *120*, 6053.

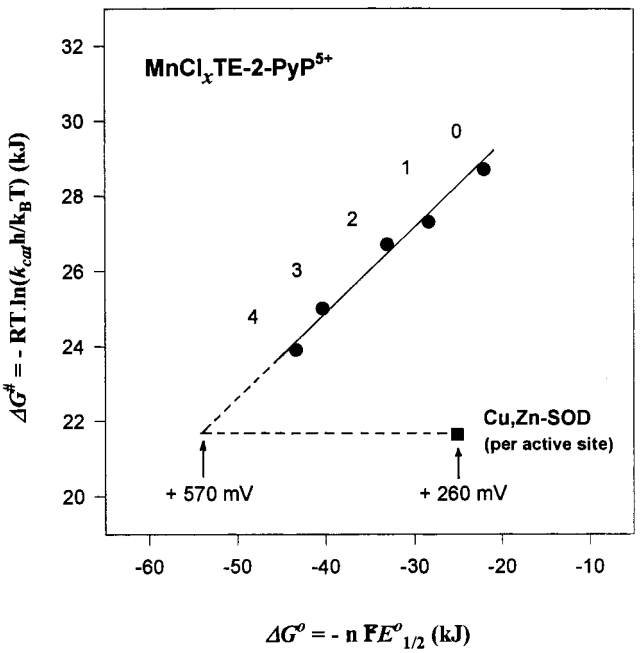

Figure 3. Plot of the free energy of activation ($\Delta G^{\ddagger}$) for the O_2^- dismutation reaction catalyzed by $MnCl_x$TE-2-PyP^{5+} as a function of the ground-state free-energy change ($\Delta G°$) for $MnCl_x$TE-2-PyP^{5+} redox. $\Delta G^{\ddagger}$ and ΔG^{o} were calculated from k_{cat} and $E°_{1/2}$ values reported in Table 3 (F, R, h, and k_B are Faraday, molar gas, Planck, and Boltzmann constants, respectively). (●) Numbers 0−4 correspond to x in $MnCl_x$TE-2-PyP^{5+}. (■) Corresponding data for one active site of Cu,Zn−SOD (ref 2).

redox state, and thus, as in the case of MnOBTMPyP^{4+}, limit the rate of the reoxidation of the metal as well as induce Mn(II) dissociation.[8,14]

Concluding Remarks

Silica-gel column chromatography, ^{1}H NMR, and mass spectrometry allowed the purification and the structural identification of H_2Cl_xT-2-PyP ($x = 1-4$). The synthesis of $MnCl_x$TE-2-PyP^{5+} allowed us to explore the relationship between superoxide dismuting activity and redox properties of such compounds. At the theoretically optimal redox potential ($E°_{1/2} \sim +360$ mV, Scheme 1), the reduction of the manganese(III) porphyrin by superoxide is apparently the rate-limiting step in the overall catalytic process. Our results raise the issue of what further chemical modifications on porphyrins would improve kinetic factors toward superoxide dismutation without affecting the stability of their manganese complexes. Because of their increased activity and their apparent good stability, $MnCl_x$TE-2-PyP^{5+} ($x = 1-4$) may be promising candidates for pharmaceutical purposes.

Abbreviations. H_2T-2-PyP, 5,10,15,20-tetrakis(2-pyridyl)porphyrin; MnTE-2-PyP^{5+}, manganese(III) 5,10,15,20-tetrakis(*N*-ethylpyridinium-2-yl)porphyrin; H_2TPP, 5,10,15,20-tetrakisphenylporphyrin; β-Cl_x, β-halogenated porphyrin with x chlorines; NCS, *N*-chlorosuccinimide; ETS, ethyl-*p*-toluenesulfonate; EDTA, ethylenedinitrilotetraacetic acid; TBAC, tetrabutylammonium chloride; SOD, superoxide dismutase; NHE, normal hydrogen electrode.

Acknowledgment. We thank Dr. M. Perrée-Fauvet (ICMO, Université de Paris-Sud, France) for her advice on porphyrin chemistry and Dr. A. L. Crumbliss (Chemistry Department, Duke University) for stimulating discussions and critical reading of the manuscript. Redox-potential measurements were performed by I. Spasojevic (Chemistry Department, Duke University). MALDI−TOFMS and ESMS mass spectra were performed by Dr. N. Srinivasan (Chemistry Department, North Carolina State University) and Dr. R. Stevens (Department of Pediatrics, Duke University), respectively. This work was supported by grants from the North Carolina Biotechnology Center Collaborative Funding Assistance Program, the National Institutes of Health, the Council for Tobacco Research-U.S.A., Inc., and Aeolus/Intercardia. R.K. also acknowledges support from the Fondation pour la Recherche Medicale (France).

IC9808854